Dalton Transactions

PAPER

View Article Online
View Journal | View Issue

Cite this: *Dalton Trans.*, 2016, **45**, 10936

High-pressure synthesis of $L1_0$ MnAl with near-stoichiometric composition

Y. Kinemuchi,* A. Fujita and K. Ozaki

Received 10th March 2016,
Accepted 2nd June 2016

DOI: 10.1039/c6dt00947f

www.rsc.org/dalton

$L1_0$ MnAl, which is a nonequilibrium ferromagnetic phase, is fabricated successfully with various compositions *via* high-pressure synthesis. The $L1_0$ phase is observed at pressures higher than 5 GPa, indicating that the volume effect is crucial for the stabilization of this phase. The employed synthesis route does not require a Mn-rich ε-phase, which has conventionally been used as the precursor compound. This allows for the synthesis of the $L1_0$ phase with a near-stoichiometric composition. In addition to variations in the composition in terms of the Mn/Al ratio, the axial ratio (c/a) as well as the ordering parameter (S) are modified systematically, with the maximum c/a and S values corresponding to the stoichiometric composition. With this structural change, the highest coercive force is also observed at the stoichiometric composition.

Introduction

Magnetic materials with high saturation magnetization (M_s) as well as large magnetic anisotropic energy (MAE) are important materials in modern society and find wide use in automotive vehicles, wind generators, and storage devices. A high M_s value can be achieved by employing the Slater–Pauling concept,[1] which involves the use of 3d elements such as Fe, Co, or Mn; however, attaining a large MAE value remains a challenge. $L1_0$-ordered binary alloys are known to have higher MAE values compared to those of disordered compounds. Among these alloys, $L1_0$ FePt shows a MAE value as high as 5 MJ m^{-3},[2,3] which is comparable to those of advanced rare-earth magnets. Basically, heavy elements such as Pt increase the MAE, owing to the enhancement in the degree of spin–orbit coupling. However, the scarcity of these elements often limits their use in practice. Thus, discovering magnetic materials composed of abundant elements is of significant technological importance. MAE values of the order of 1–2 MJ m^{-3} have been reported for the compounds FeNi,[4] CoNi,[5] MnAl,[6] and MnGa,[7] of which MnAl is regarded as being more cost-effective and comparable or superior to hard ferrites and alnicos.[8]

$L1_0$ MnAl can be considered as having a body-centered tetragonal structure and has been synthesized by using the ε-phase (hcp) as the mother phase. The ε-phase is a Mn-rich (typical composition of $Mn_{0.55}Al_{0.45}$) high-temperature phase that is stable at temperatures greater than 873 °C. The quenching of the ε-phase and its subsequent annealing (typically at approximately 500 °C) results in the formation of the $L1_0$ phase.[9] $L1_0$ MnAl is known to decompose into nonmagnetic phases and is thus regarded as a metastable phase. In addition, synthesized MnAl compounds have a non-stoichiometric composition that deviates from the ideal one (Mn_1Al_1), depending on the synthesis route used. The excess Mn must occupy an antisite (Al site), which leads to antiferromagnetic (AFM) coupling with the Mn site and thus a decrease in the M_s value.

Historically, $L1_0$ MnAl has been considered a product formed by the displacive or martensitic transformation of the ε-phase.[10] However, a detailed analysis performed using high-resolution transmission electron microscopy revealed that the growth front of the $L1_0$ phase is compositionally invariant with regard to the ε-phase that can be regarded as the mother phase. Furthermore, although the $L1_0$ phase nucleates heterogeneously at the previously existing ε-phase grain boundary, it forms incoherent interfaces.[11] Hence, the proposed displacive or martensitic transformation must be discarded as the underlying mechanism. In other words, the formation of the ε-phase is not a necessary condition for the formation of the $L1_0$ phase.

The intrinsic properties of the $L1_0$ phase have been examined extensively using density functional theory (DFT). According to previous DFT studies, the M_s value of the $L1_0$ phase is 2.4μ_B per u.c., while its MAE value is 1.5–1.8 MJ m^{-3}.[12–14] It has also been predicted that extending the axial ratio (c/a) increases the MAE value.[13] On the experimental side, however, pure MnAl has not yet been synthesized,

National Institute of Advanced Industrial and Science and Technology (AIST), Nagoya 463-8560, Japan. E-mail: y.kinemuchi@aist.go.jp

owing to issues related to the synthesis method used, as mentioned earlier. Thus, the M_s value is lower than the theoretical value ($1.9\mu_B$ per u.c.).[9] Therefore, there is a need to develop an alternative synthesis route that does not require the ε-phase.

It is interesting to note that the $L1_0$ MnAl phase possesses the smallest unit cell among all the phases near the stoichiometric composition in this system. Hence, the volume effect is thought to stabilize the $L1_0$ phase. In the present work, the high-pressure synthesis (HPS) of $L1_0$ MnAl was performed as an alternative synthesis route. Furthermore, the effects of the composition on the $L1_0$ structure as well as the resultant magnetic properties are discussed.

Experimental

The source materials, Mn (3Nup, 300 μm passed powder, Kojundo Chemical Laboratory Co., Ltd Japan) and Al (2Nup, 300 μm passed powder, Kojundo Chemical Laboratory Co., Ltd Japan), were homogeneously mixed using a planetary mixing apparatus, and the mixture was subsequently pelletized in a cylindrical form. Next, these pellets were placed in an Al_2O_3 crucible and melted in a furnace filled with a mixture of 5% H_2/Ar at 1300 °C for 10 min. After being melted, the samples were crushed into a course powder using a vibration milling apparatus made of tungsten carbide. The powder obtained was used as the source material for the HPS process. We confirmed that the source materials were alloyed homogeneously and resulted in compounds corresponding to the phase diagrams:[15] those corresponding to the formation of γ_2 ($R3m$) and/or β-Mn ($P4_132$) phases, depending on the composition.

The HPS process was performed using a cubic anvil setup. The source materials were pelletized into cylinders with a diameter of 4.3 mm and a length of 6.2 mm. These small pellets were placed in a gold capsule, in order to prevent them from being contaminated during the synthesis process. Pyrophyllite was used as the pressure medium. Prior to the start of the experiments, the pressure acting on the sample was calibrated based on the phase transitions of Bi and Ba. The temperature was raised once the pressure had reached the desired level. It was then held at that level for 1 h and subsequently reduced while the pressure was maintained. Finally, the pressure was released once the temperature had dropped to room temperature. Typical samples after the HPS had dimensions of 4 mm in diameter and 4 mm in length.

The sample composition was analyzed using an energy-dispersive X-ray fluorescence spectrometer (EDX-8000, Shimadzu, Japan, for the average composition; and Quantax 70, Bruker AXS Japan, for the microanalysis). The X-ray powder diffraction pattern was obtained using parallel beam optics (RINT 2000, Rigaku, Japan). The pattern was then investigated using Rietveld analysis (Rietan 2000).[16] The fraction of the product phases was estimated from the scale factors optimized in the Rietveld analysis. The ordering parameter (S) of the $L1_0$ phase was deduced from the relative intensity of the superlattice ($h + k + l$ = odd) and fundamental ($h + k + l$ = even):

$$S = \sqrt{\frac{I_S/I_F|_{obs}}{I_S/I_F|_{cal}}}$$

here I_F and I_S are the intensities of fundamental peaks and superlattice peaks, respectively.

The magnetic properties at room temperature were measured using a physical property measurement system (PPMS, Quantum Design Co.) equipped with a vibrating sample magnetometer.

Results and discussion

During conventional synthesis, the $L1_0$ phase emerges during annealing at approximately 500 °C. However, the effects of pressure at this temperature are not observed. Hence, the HPS process was performed at a higher temperature such as 900 °C. This increase in the HPS process temperature had a dramatic impact on $L1_0$ formation, as shown in Fig. 1. At pressures lower than 5 GPa, the γ_2- and β-phases, that is, the phases that are stable under atmospheric conditions, still existed. On further increasing the pressure, a transformation to the $L1_0$ phase was observed clearly, and so was a gradual increase in the phase fraction. However, we did not succeed in eliminating the secondary phase even after applying the maximum pressure that the apparatus used allowed (9 GPa). Nevertheless, it is clear that the pressure effect, that is, a reduction in the volume, is the key to stabilizing the $L1_0$ phase. This newly discovered synthesis route contradicts conventional wisdom in that the ferromagnetic (FM) phase preferentially exhibits an increase in volume. When the distance between magnetic atoms is small, it tends to result in AFM coupling.[17] Thus, the HPS process has not been used for the synthesis of ferromagnetic phases. Hence, it was interesting to

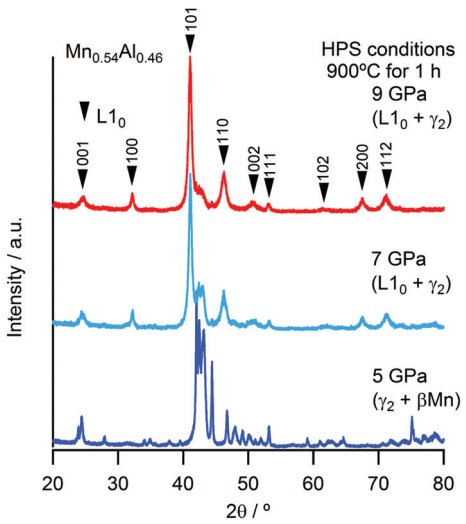

Fig. 1 Effect of pressure on the formation of the $L1_0$ phase.

determine the Mn–Mn distances in this system. At the nominal stoichiometric composition of MnAl, $L1_0$ competes with the γ_2-phase, which has a Cr_5Al_8-type structure (space group of *R*3*m*) composed of several icosahedra. The smallest Mn–Mn distance in the γ_2-phase is 2.59 Å, which is much shorter than that of $L1_0$ (2.75 Å). As expected on the basis of this distance, the γ_2-phase is an AFM compound. On the other hand, the γ_2-phase exhibits a longer length for the Al–Al bond. With respect to the Al–Mn bonds, even though their length exhibits a wide distribution, they are basically comparable to or longer than those in the $L1_0$ phase. The fact that the Al atoms are dispersed with respect to the Mn atoms as well as with respect to the other Al atoms leads to the density of the γ_2-phase being lower than that of the $L1_0$ phase. In other words, the pressure compresses the dispersed Al atoms. Meanwhile, the Mn–Al distance also reduces and eventually the approached Al starts to interfere with the Mn–Mn bonds, resulting in the emergence of an FM phase owing to the increase in the Mn–Mn bond length. Although this simple explanation does not account for the mechanism of ordering, it may open a new perspective for finding FM phases.

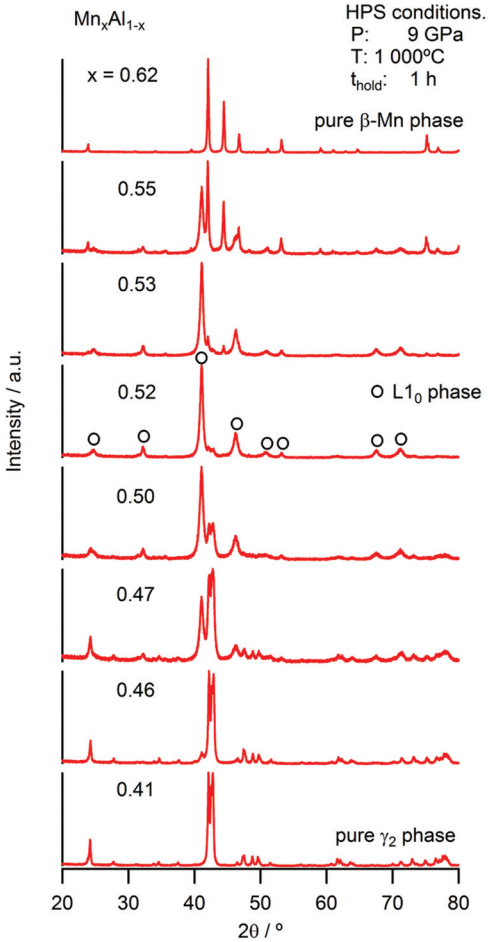

Fig. 2 Variations in the constituent phases for various compositions after the HPS process.

Fig. 2 shows the strong effect of compositional variation on the constituent phases. With the increase in the Mn content, the $L1_0$ phase becomes stable instead of the γ_2-phase, with the β-phases eventually becoming stable. In addition, Mn composition denoted as *x* corresponds to that of the sample: the averaged Mn content among the product phases. Fig. 3 shows the images of compositional mapping of a $Mn_{0.52}Al_{0.48}$ sample. The Mn rich phase exists as a secondary phase. On the other hand, the composition of the $L1_0$ phase was found to be similar to the average composition within the analytical variation of EDS. A similar trend was found for the other samples: the composition of $L1_0$ was the same as the average composition. The highest fraction of $L1_0$, which was approximately 90%, was found when the composition was slightly rich in Mn (0.52 at%); this concentration of Mn is still lower than that corresponding to the conventional synthesis route based on the ε-phase (approximately 0.54 at%) (see Fig. 4). In terms of the chemical ordering, the ordering parameter (*S*) as well as site occupancy at 1a and 1d sites were deduced (Fig. 5 and Table 1). As demonstrated in both analyses, chemical ordering was rationally dependent on the composition—the stoichiometric composition is crucial for the high degree of ordering.

The lattice parameters of the $L1_0$ phases are listed in Fig. 6. Although the cell volume was almost constant for all the compositions, the axial length, *c*, was the maximum at the stoichiometric composition, while the *a*-axis was the minimum. As a

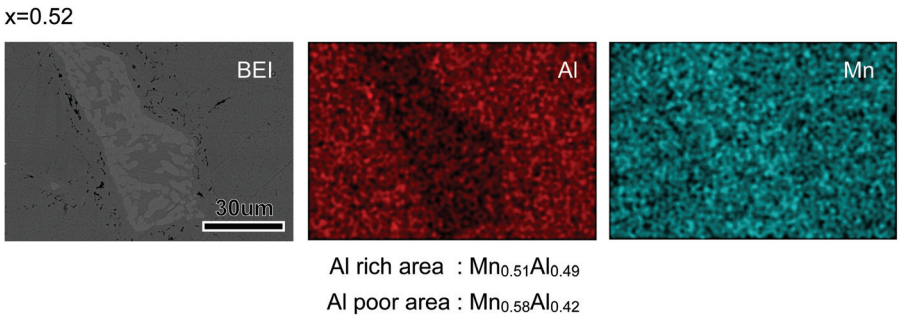

Fig. 3 Microstructural images of a $Mn_{0.52}Al_{0.48}$ sample. Back-scattered electron image (BEI), EDS mapping images of Al (Al) and Mn (Mn). The compositions corresponding to Al rich/poor areas are also noted. The variation of the composition was found to be 1 at%.

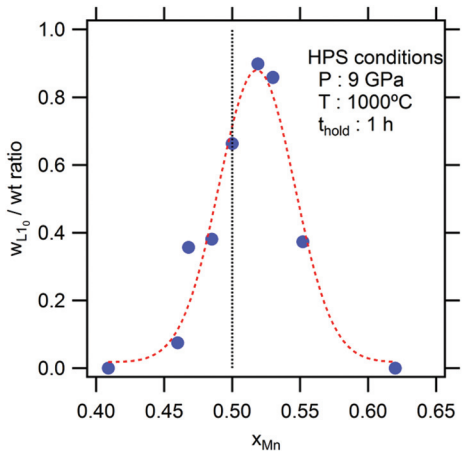

Fig. 4 Phase fraction of $L1_0$ for various compositions. The line is a visual guide.

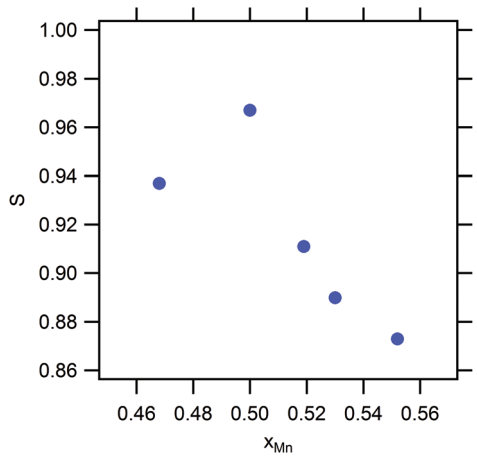

Fig. 5 Ordering parameter (S) of $L1_0$ phases for various compositions.

Table 1 Site occupancy of Mn_xAl_{1-x}

	1a (0 0 0)		1d (1/2 1/2 1/2)	
x	Mn	Al	Mn	Al
0.47	0.932	0.068	0.008	0.992
0.50	0.993	0.007	0.007	0.993
0.52	0.995	0.005	0.045	0.955
0.53	0.994	0.006	0.066	0.934
0.55	0.986	0.014	0.114	0.886

result, the axial ratio, c/a, was the highest value at this composition. This trend is conventionally thought to originate due to the decrease in the extent of Mn occupancy at the antisites in the case of the Mn-rich compositions, resulting in an increase in the c-axis length owing to the reduction in AFM coupling.

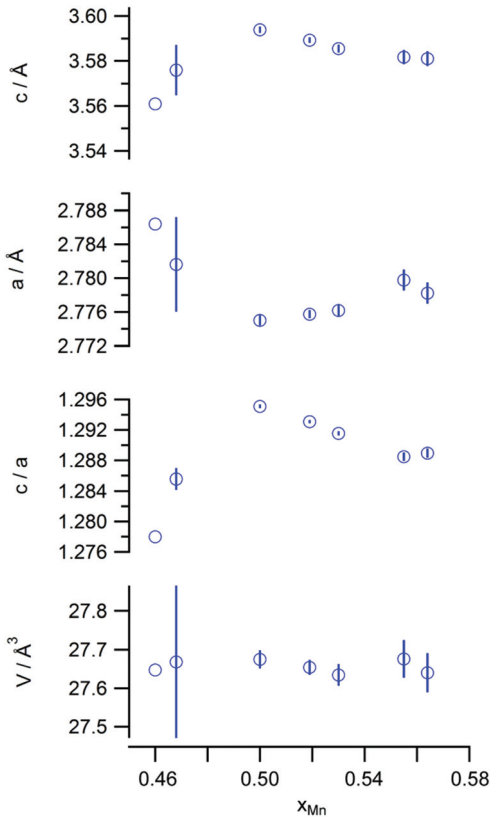

Fig. 6 Lattice constants (c and a), axial ratio (c/a), and cell volume (V) values of the $L1_0$ phases.

On the other hand, the c/a value also decreased when the amount of Al was excessive. In an early DFT study, Sakuma pointed out that the tetragonal distortion resulting from the transformation of the cubic B2 structure into the $L1_0$ structure results in the splitting of the d bands, owing to the destruction of the degeneracy at the Fermi level, and suggested the existence of the solid-state Jahn–Teller effect in this system.[7] Later, the structural stability of this system was investigated based on DFT. It was found that nonmagnetic MnAl preferentially forms a cubic B2 structure, highlighting the importance of magnetic interaction in the structure.[18] In short, the FM state prefers the tetragonal $L1_0$ structure, and the tetragonality is expected to be weakened with a reduction in the magnetic moment. Thus, the reduction in tetragonality with the increase in the nonmagnetic Al content can be explained on this basis.

The typical magnetization curves of the test samples are shown in Fig. 7. Owing to the difference in the $L1_0$ contents, the saturation magnetization (M_s) varied from sample to sample, while the coercive force (H_c) values of the samples were almost similar. These are plotted against the Mn content in Fig. 8. The highest M_s value was observed in the case of a slightly Mn-rich composition, for which the volume extent of the $L1_0$ phase in the product was the highest. In order to account for the effect of the secondary phases, the observed M_s value was normalized with respect to the $L1_0$ phase weight

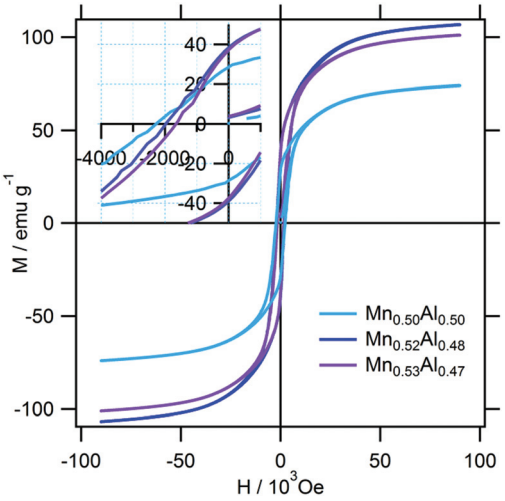

Fig. 7 Typical magnetization curves. The inset shows a magnified image of the area near the origin.

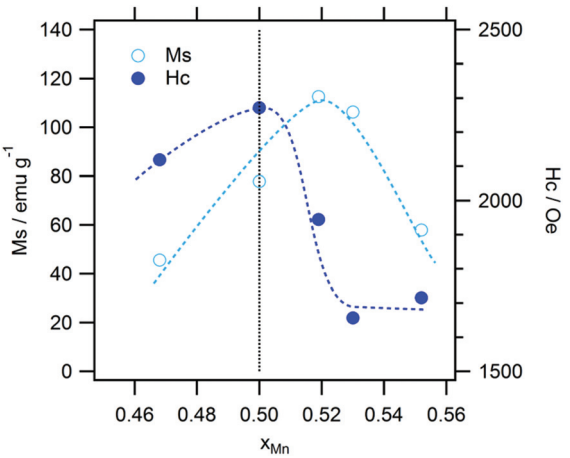

Fig. 8 Saturation magnetization (M_s) and coercive force (H_c) values. The lines are a visual guide.

fraction, which was evaluated as being $1.8\mu_B$ for the samples. This value corresponds to 75% of the theoretical one. In addition, we expected that the normalization would increase the M_s towards the stoichiometric composition. However, this trend was not observed, so that the ordering parameter did not matter either. On the other hand, the highest H_c value was observed at the stoichiometric composition. A plot of H_c against the axial ratio (c/a) (see Fig. 9) shows that the increase in tetragonality increased H_c. It is interesting to note that the reduction in c/a did not significantly decrease H_c in the case of the Al-rich composition.

The effect of c/a on the MAE value of several $L1_0$ compounds has been investigated theoretically using a second-order perturbation formula.[13] According to the obtained results, the MAE value of $L1_0$ compounds tends to become higher with the c/a value. This can be roughly explained from

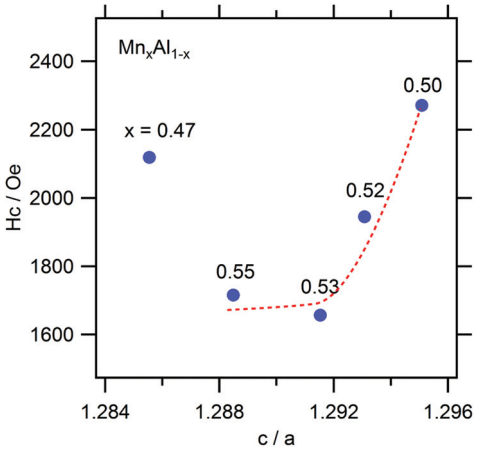

Fig. 9 Coercive force (H_c) as a function of the axial ratio (c/a). The guiding line represents Mn-rich samples.

that the reduction in the dimensionality results in localized valence electrons, leading to the increase in the gradient in the electrostatic potential and subsequent strengthening in the spin–orbit interactions. More specifically, for the MnAl system, an increase in the MAE value of approximately 18% is predicted for an increase in c/a of 5%. The theory reasonably explains the obtained experimental results; however, the degree of quantitative agreement is rather low. In the present work, an increase in H_c of 37% was caused by a mere difference of 0.3% in c/a. This suggests that the Mn present at the antisite was the dominant factor affecting MAE: the ordering was more critical than the c/a in the case of the studied samples. Indeed, we found a linear relationship between H_c and S among the samples (Fig. 10). In addition, the rough estimation of the anisotropic field based on the initial magnetization and corresponding differential curves showed a marginal difference among them, which suggests that the

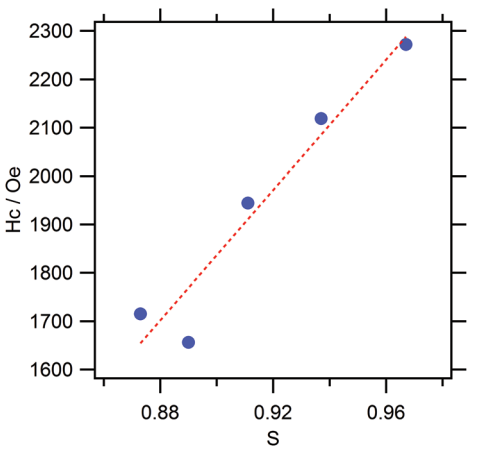

Fig. 10 Coercive force (H_c) against ordering parameter (S). The lines are a visual guide.

microstructural influence was observed in the H_c of present samples as well.

Conclusions

The HPS process was used for the synthesis of the $L1_0$ MnAl phase, resulting in the emergence of $L1_0$ at pressures higher than 5 GPa at 900 °C. The increase in the phase fraction with the pressure indicated that the $L1_0$ phase forms preferentially at small volumes. In contrast to the conventional synthesis method, which is based on the use of the ε-phase, the proposed synthesis route was found to be advantageous in terms of the fact that various compositional Mn/Al ratios, including the stoichiometric composition, could be attained. The structural analysis of the $L1_0$ phases revealed that the lattice constants varied systematically with the composition, with the highest c/a and S values being observed at the stoichiometric composition. The maximum M_s value was observed at a slightly Mn-rich composition; this was because the fraction of the $L1_0$ phase in the product was the highest in this case. In addition, the M_s value normalized with respect to the $L1_0$ fraction was estimated to be $1.8\mu_B$, which was 75% of the theoretical one. On the other hand, H_c tended to increase with S and reached its maximum at the stoichiometric composition. The change in H_c with S suggests that the elimination of Mn at the antisite is crucial.

Acknowledgements

This paper is based on the results obtained during the Future Pioneering Program "Development of magnetic material technology for high-efficiency motors", which was commissioned by the New Energy and Industrial Technology Development Organization (NEDO), Japan.

References

1 J. C. Slater, *J. Appl. Phys.*, 1937, **8**, 385.
2 S. Okamoto, N. Kikuchi, O. Kitakami, T. Miyazaki, Y. Shimada and K. Fukamichi, *Phys. Rev. B: Condens. Matter*, 2002, **66**, 024413.
3 P. Ravindran, A. Kjekshus, H. Fjellvåg, P. James, L. Nordström, B. Johansson and O. Eriksson, *Phys. Rev. B: Condens. Matter*, 2001, **63**, 144409.
4 Y. Miura, S. Ozaki, Y. Kuwabara, M. Tsujikawa, K. Abe and M. Shirai, *J. Phys.: Condens. Matter*, 2013, **25**, 106005.
5 S. Fukami, H. Sato, M. Yamanouchi, S. Ikeda and H. Ohno, *Appl. Phys. Express*, 2013, **6**, 073010.
6 S. H. Nie, L. J. Zhu, J. Lu, D. Pan, H. L. Wang, X. Z. Yu, J. X. Xiao and J. H. Zhao, *Appl. Phys. Lett.*, 2013, **102**, 152405.
7 A. Sakuma, *J. Magn. Magn. Mater.*, 1998, **187**, 105.
8 J. M. Coey, *J. Phys.: Condens. Matter*, 2014, **26**, 064211.
9 J. Z. Wei, Z. G. Song, Y. B. Yang, S. Q. Liu, H. L. Du, J. Z. Han, D. Zhou, C. S. Wang, Y. C. Yang, A. Franz, D. Többens and J. B. Yang, *AIP Adv.*, 2014, **4**, 127113.
10 J. J. Van Den Broek, H. Donkersloot, G. Van Tendeloo and J. Van Landuyt, *Acta Metall.*, 1979, **27**, 1497.
11 C. Yanar, J. M. K. Wiezorek, V. Radmilovic and W. A. Soffa, *Metall. Mater. Trans. A*, 2002, **33**, 2413.
12 A. Sakuma, *J. Phys. Soc. Jpn.*, 1994, **63**, 1422.
13 T. Kosugi, T. Miyake and S. Ishibashi, *J. Phys. Soc. Jpn.*, 2014, **83**, 044707.
14 A. Edström, J. Chico, A. Jakobsson, A. Bergman and J. Rusz, *Phys. Rev. B: Condens. Matter*, 2014, **90**, 014402.
15 M. Ellner, *Metall. Trans. A*, 1990, **21**, 1669.
16 F. Izumi and K. Momma, *Solid State Phenom.*, 2007, **130**, 15.
17 E. Şaşioğlu, L. M. Sandratskii and P. Bruno, *Phys. Rev. B: Condens. Matter*, 2005, **71**, 214412.
18 Y. Kurtulus and R. Dronskowski, *J. Solid State Chem.*, 2003, **176**, 390.